

Frame dependence of transition form factors in light-front dynamics

Meijian Li,^{1,*} Yang Li,^{1,2,3,†} Pieter Maris,^{1,‡} and James P. Vary^{1,§}

¹*Department of Physics and Astronomy, Iowa State University, Ames, IA, 50011*

²*Hebei Key Laboratory of Compact Fusion, Langfang 065001, China*

³*ENN Science and Technology Development Co., Ltd., Langfang 065001, China*

(Dated: August 19, 2019)

We calculate the transition form factor between vector and pseudoscalar quarkonia in both the timelike and the spacelike region using light-front dynamics. We investigate the frame dependence of the form factors for heavy quarkonia with light-front wavefunctions calculated from the valence Fock sector. This dependence could serve as a measure for the Lorentz symmetry violation arising from the Fock-space truncation. We suggest using frames with minimal longitudinal momentum transfer for calculations in the valence Fock sector, namely the Drell-Yan frame for the space-like region and a specific longitudinal frame for the timelike region; at $q^2 = 0$ these two frames give the same result. We also use the transition form factor in the timelike region to investigate the electromagnetic Dalitz decay $\psi_A \rightarrow \psi_B l^+ l^-$ ($l = e, \mu$) and predict the effective mass spectrum of the lepton pair.

I. INTRODUCTION

The electromagnetic (EM) transition between quarkonium states, which occurs via emission of a photon, $\psi_A \rightarrow \psi_B \gamma$, offers insights into the internal structure and the dynamics of such systems. The magnetic dipole (M1) transition, which takes place between pseudoscalar and vector mesons ($\psi_A, \psi_B = \mathcal{V}, \mathcal{P}$ or \mathcal{P}, \mathcal{V}), has been detected with strong signals [1] and stimulates various theoretical investigations [2–6]. Similarly, the EM Dalitz decay [7], $\psi_A \rightarrow \psi_B l^+ l^-$, can be treated by coupling a virtual photon to the final lepton pair. The Dalitz decay, also known as the leptonic conversion decay, provides additional information about the meson structure owing to the virtual photon kinematics. Though widely observed in the light meson sector, such as $\phi \rightarrow \pi^0 e^+ e^-$ [8], $\phi \rightarrow \eta e^+ e^-$ [9, 10], and $\omega \rightarrow \pi^0 e^+ e^-$ [11, 12], only a few such decays have been detected in the heavy sector. The observed Dalitz decays of quarkonium are decays to a light meson plus a lepton pair, such as $J/\psi \rightarrow \eta e^+ e^-$, $J/\psi \rightarrow \eta' e^+ e^-$ [13], and $\psi(3686) \rightarrow \eta' e^+ e^-$ [14]. We investigate the M1 EM Dalitz decay with initial and final mesons both being heavy quarkonia, in the hope of providing another probe of the interaction of quarkonium states with photons.

The roles of the underlying strong dynamics in those processes are encoded within the q^2 -dependent transition form factor $V(q^2)$, which arises from the Lorentz structure decomposition of the hadron matrix element $\langle \psi_B(P) | J^\mu(0) | \psi_A(P' = P + q) \rangle$. q^2 is the square of the momentum transfer between ψ_A and ψ_B , and is also the square of the invariant mass of the lepton pair in the Dalitz decay.

The transition form factor is Lorentz invariant—it should not depend on the choice of the current components or the reference frames. In general, in light-front dynamics, the transition form factor receives two major contributions, a parton-

number-conserving term where the photon couples to a parton, and a parton-number-non-conserving term where a quark-antiquark pair from the initial state annihilates into a photon, as illustrated in Fig. 1. Each diagram could contribute dif-

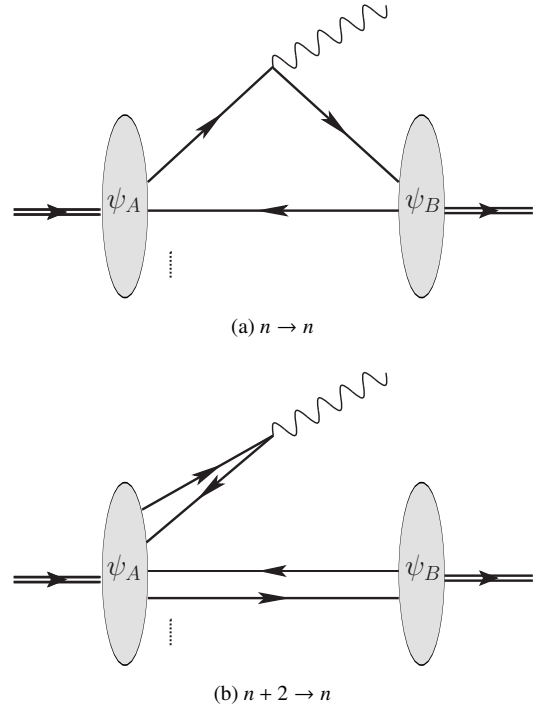


FIG. 1. The two dominant contributions to the transition $\psi_A \rightarrow \psi_B \gamma^{(*)}$ on the light front: (a) the parton-number-conserving term, and (b) the parton-number-non-conserving term. Diagrams are light-front time ordered. Light-front time flows from the left to the right.

ferently when a different current component is used or a different frame is chosen [15–18]. In practical calculations the Fock space is truncated, so we only have access to part of the contributions. For instance, if the light-front wavefunctions of the mesons are solved in a truncation retaining only the valence Fock sector, contributions like Fig. 1(b) cannot be ac-

* meijianl@iastate.edu
 † leeyoung@iastate.edu
 ‡ pmaris@iastate.edu
 § jvary@iastate.edu

cessed directly¹. The transition form factor is evaluated from the available finite Fock space, and a dependence on the current components or the frames could arise. In such situations, knowing the current or frame dependence could help quantify theoretical uncertainties. One further issue to resolve is whether there exists a preferred current or a preferred frame such that the neglected contributions from higher Fock sectors could be minimized.

Dependence on current components when extracting the elastic and transition form factors on the light front has been studied extensively for various systems and theories [16, 17, 19–21]. The J^+ current has gained the reputation as the “good current” for the simplicity in evaluating the elastic form factor in the spacelike region in the Drell-Yan frame. The covariant formulation of light-front dynamics (CLFD) provides a procedure to unambiguously extract the transition form factors in the Drell-Yan frame (see Ref. [19] for a review). To explore some alternatives, we investigated the M1 transition form factor through different current components (J^+ and J^\perp) and different magnetic projections ($m_j = 0, \pm 1$) of the vector meson [22]. There, we have shown that, at least in the context of heavy quarkonia with valence Fock sector light-front wavefunctions, using the transverse current J^\perp in conjunction with the $m_j = 0$ state of the vector meson is preferred to other choices. With the transverse current echoing the 3-dimensional current density operator, this choice employs the dominant spin components of the light-front wavefunctions, and connects well with the non-relativistic limit of the heavy system. While this preference applies to any choice of frame, the calculation of the final results was carried out in the Drell-Yan frame [22].

It is the purpose of this work to further investigate the frame dependence of transition form factors. Studies in the literature have revealed that the elastic and transition form factors could have different results when evaluated in different reference frames [17, 18, 23–25]. Such frame dependence is closely related to the Fock-space truncation that omits the non-valence contributions. In this work, instead of looking into a few selective frames, we sample all frames with the same q^2 .

In particular, we sample various frames by allowing the transferred momentum q^2 to be apportioned between the longitudinal direction and the transverse direction. For example, in the Drell-Yan frame ($q^+ = 0$), all the transferred momentum is in the transverse direction and none in the longitudinal, providing one limit to our frame selection. The other limit is referred to as the longitudinal frame, where q^2 is solely in the longitudinal direction. We decompose q^2 into two boost invariants [see Eq. (4)]. Due to the boost invariance in light-front dynamics, each of these frames represents infinitely many frames related by light-front boosts. Our work explores the full range of frame dependence that is implicit in the adopted light-front model for the systems investigated here.

By analyzing the light-front wavefunction representation of the hadron matrix elements, we find that frames with minimal longitudinal momentum transfer could suppress non-valence contributions, and are thus preferred for calculations in the valence Fock sector. Those are, the Drell-Yan frame in the space-like region, and the longitudinal-II frame in the time-like region, as defined in Sec. II. Our suggested frames agree with the study by Bakker and collaborators on the semileptonic decay [18]. In their work, the transition form factor in the time-like region obtained from one specific frame in the valence Fock sector is closest to the full solution that also includes non-valence contributions. This specific frame is defined as $\vec{q}_\perp = 0$ with negative recoil, which resembles the longitudinal-II frame in this work.

As in our previous study on the radiative decays [22], here we employ the light-front wave functions of the heavy quarkonia from the basis light-front quantization (BLFQ) approach [26]. The effective Hamiltonian is based on light-front holographic QCD and the one-gluon exchange light-front QCD interaction [27, 28]. We find that the frame dependence of the transition form factor can be characterized as ranging between two limiting cases, similar to the dependence shown for the elastic form factor of (pseudo-)scalar mesons [25]. The spread of this frame dependence could serve as a measure for the violation of the Lorentz symmetry due to Fock space truncation.

The layout of this paper is as follows. In Sec. II, we introduce the formalism and methods to calculate the M1 transition form factor with general frames on the light front. We then apply the formalism to heavy quarkonia in the Basis Light Front Quantization (BLFQ) approach in Sec. III and there we present the results of the transition form factors from different frames and the effective mass spectrum for the resulting lepton pair in the Dalitz decay. We summarize our paper in Sec. IV.

II. TRANSITIONS ON THE LIGHT FRONT

A. The decay width

The Lorentz covariant decomposition of the electromagnetic transition matrix element between a vector meson (\mathcal{V}) and a pseudoscalar (\mathcal{P}) is [29]

$$\langle \mathcal{P}(P) | J^\mu(0) | \mathcal{V}(P', m_j) \rangle = \frac{2V(q^2)}{m_{\mathcal{P}} + m_{\mathcal{V}}} \epsilon^{\mu\alpha\beta\sigma} P_\alpha P'_\beta e_\sigma(P', m_j), \quad (1)$$

where $q^\mu = P'^\mu - P^\mu$ represents the momentum transfer between the initial and final mesons. On the light front, $\mu = +, -, x, y$ ($v^\pm = v^0 \pm v^z$, we use the same conventions of the light-front coordinate as in Ref. [22]). $V(q^2)$ is the transition form factor. $m_{\mathcal{P}}$ and $m_{\mathcal{V}}$ are the masses of the pseudoscalar and the vector, respectively. e_σ is the polarization vector of the vector meson, with $m_j (= 0, \pm 1)$ the magnetic projection.

In the process of $\psi_A \rightarrow \psi_B \gamma$, ($\psi_A, \psi_B = \mathcal{V}, \mathcal{P}$ or \mathcal{P}, \mathcal{V}), $q^2 = 0$, the decay width in the rest frame of the initial particle

¹ In principle, evaluation of observables in a truncated Fock space requires a renormalization of the operator. We omit such a renormalization in the present work.

could be derived from the transition matrix element [22],

$$\Gamma(\psi_A \rightarrow \psi_B \gamma) = \frac{(m_A^2 - m_B^2)^3}{(2m_A)^3 (m_A + m_B)^2} \frac{|V(0)|^2}{(2J_A + 1)\pi}. \quad (2)$$

J_A is the angular momentum of the initial meson ψ_A .

For the Dalitz decay $\psi_A \rightarrow \psi_B l^+ l^-$, the physical region of interest is $4m_l^2 \leq q^2 \leq (m_A - m_B)^2$. The effective mass spectrum of the lepton pair could be derived as [30]:

$$\frac{d\Gamma(\psi_A \rightarrow \psi_B l^+ l^-)}{dq^2 \cdot \Gamma(\psi_A \rightarrow \psi_B \gamma)} = \frac{\alpha}{3\pi} \sqrt{1 - \frac{4m_l^2}{q^2}} \left(1 + \frac{2m_l^2}{q^2}\right) \frac{1}{q^2} \times \left[\left(1 + \frac{q^2}{m_A^2 - m_B^2}\right)^2 - \frac{4m_A^2 q^2}{(m_A^2 - m_B^2)^2} \right]^{3/2} \left| \frac{V(q^2)}{V(0)} \right|^2. \quad (3)$$

B. Frames and kinematics

Considering the transition $\psi_A(P') \rightarrow \psi_B(P)\gamma^{(*)}(q = P' - P)$, the Lorentz invariant momentum transfer q^2 can be written as a function of two boost invariants [25] according to four-momentum conservation $q^2 = (P' - P)^2$,

$$q^2 = zm_A^2 - \frac{z}{1-z}m_B^2 - \frac{1}{1-z}\vec{\Delta}_\perp^2. \quad (4)$$

where,

$$z \equiv (P'^+ - P^+)/P'^+, \quad \vec{\Delta}_\perp \equiv \vec{q}_\perp - z\vec{P}'_\perp.$$

z can be interpreted as the relative momentum transfer in the longitudinal direction, and $\vec{\Delta}_\perp$ describes the momentum transfer in the transverse direction. Note that z is restricted to $0 \leq z < 1$ by definition. For each possible value of q^2 , the values of the pair $(z, \vec{\Delta}_\perp)$ are not unique, and those different choices correspond to different reference frames (up to longitudinal and transverse light-front boost transformations). Fig. 2 should help visualize the functional form of $q^2(z, \vec{\Delta}_\perp)$. Since q^2 is relevant to the magnitude of $\vec{\Delta}_\perp$ but not its angle, we plot it in the $\arg \vec{\Delta}_\perp = 0, \pi$ plane. Transition form factors evaluated at different $(z, \vec{\Delta}_\perp)$ but at the same q^2 could reveal the frame dependence. In particular, we introduce two special frames for detailed consideration.

- Drell-Yan frame ($z = 0$): $q^+ = 0$, $\vec{\Delta}_\perp = \vec{q}_\perp$ and $q^2 = -\vec{\Delta}_\perp^2$. This frame is shown as a single thick solid line in each panel of Fig. 2. The Drell-Yan frame is conventionally used together with the plus current J^+ to calculate the electromagnetic form factors. This choice, on the one hand, avoids spurious effects related to the orientation of the null hyperplane where the light-front wavefunction is defined and, on the other hand, it suppresses the contributions from the often-neglected

pair creation process, at least for pseudoscalar mesons [16, 17, 19–21, 31]. For the transition form factor, this is only true if zero-mode contributions are neglected. The transition form factor obtained in the Drell-Yan frame is significantly restricted in the space-like region, i.e. $q^2 \leq 0$. Although one could analytically continue the form factor to the time-like region by changing \vec{q}_\perp to $i\vec{q}_\perp$ [18, 32, 33], we elect to calculate transition form factors directly from wavefunctions.

- longitudinal frame ($\vec{\Delta}_\perp = 0$): $q^2 = zm_A^2 - zm_B^2/(1-z)$. Note that we use the same definition for the longitudinal frame as in Ref. [25], which is different from those in the literature where $\vec{q}_\perp = 0$ is called the longitudinal frame [15, 17, 18, 34]. In this frame, we have access to the kinematic region up to $q_{\max}^2 = (m_A - m_B)^2$, the point where the final meson does not recoil. This maximal value occurs at $z = 1 - m_B/m_A \equiv z_{\text{turn}}$. For a given q^2 , there are two solutions for z , corresponding to either positive or negative recoil direction of the final meson relative to the initial meson, namely,

$$\text{- longitudinal-I: } z = \frac{[m_A^2 - m_B^2 + q^2 + \sqrt{(m_A^2 - m_B^2 + q^2)^2 - 4m_A^2 q^2}]/(2m_A^2)}{1 - z_{\text{turn}}}. \quad z_{\text{turn}} \leq z < 1.$$

This branch joins the second branch at $q^2 = q_{\max}^2$ with $z = z_{\text{turn}}$, $\vec{\Delta}_\perp = 0$. The time-like region is accessed at $z_{\text{turn}} \leq z < z_{\text{node}}$, and the space-like region is at $z_{\text{node}} \leq z < 1$, where $z_{\text{node}} \equiv 1 - m_B^2/m_A^2$. The longitudinal-I frame is shown as thick dotted lines in Fig. 2.

$$\text{- longitudinal-II: } z = \frac{[m_A^2 - m_B^2 + q^2 - \sqrt{(m_A^2 - m_B^2 + q^2)^2 - 4m_A^2 q^2}]/(2m_A^2)}{1 - z_{\text{turn}}}. \quad 0 \leq z \leq z_{\text{turn}}.$$

This second branch only exists in the time-like region, and it joins the Drell-Yan frame at $q^2 = 0$ with $z = 0$, $\vec{\Delta}_\perp = 0$. The longitudinal-II frame is shown as thick dashed lines in Fig. 2.

C. Light-front wavefunction representation of the M1 transition form factor

The meson state vector $|\psi_h(P, j, m_j)\rangle$ can be expanded in the light-front Fock space. The coefficients of the Fock expansion are the complete set of n -particle light-front wavefunctions (LFWFs), $\{\psi_{n/h}^{(m_j)}(x_i, \vec{k}_{i\perp}, s_i)\}$. $x_i \equiv \kappa_i^+/P^+$ is the longitudinal momentum fraction of the i -th parton, and $\vec{k}_{i\perp} \equiv \vec{\kappa}_{i\perp} - x\vec{P}_\perp$ is the relative transverse momenta, with κ_i being the momenta of the corresponding parton. s is the spin of the parton.

The transition amplitude $\psi_A \rightarrow \psi_B \gamma^{(*)}$ is given by the sum of the diagonal $n \rightarrow n$ and off-diagonal $n + 2 \rightarrow n$ transitions, as shown in Fig. 1. For the $n \rightarrow n$ term, as in Fig. 1(a), the external photon is coupled to a quark or an antiquark, thus the electromagnetic current matrix element takes the form

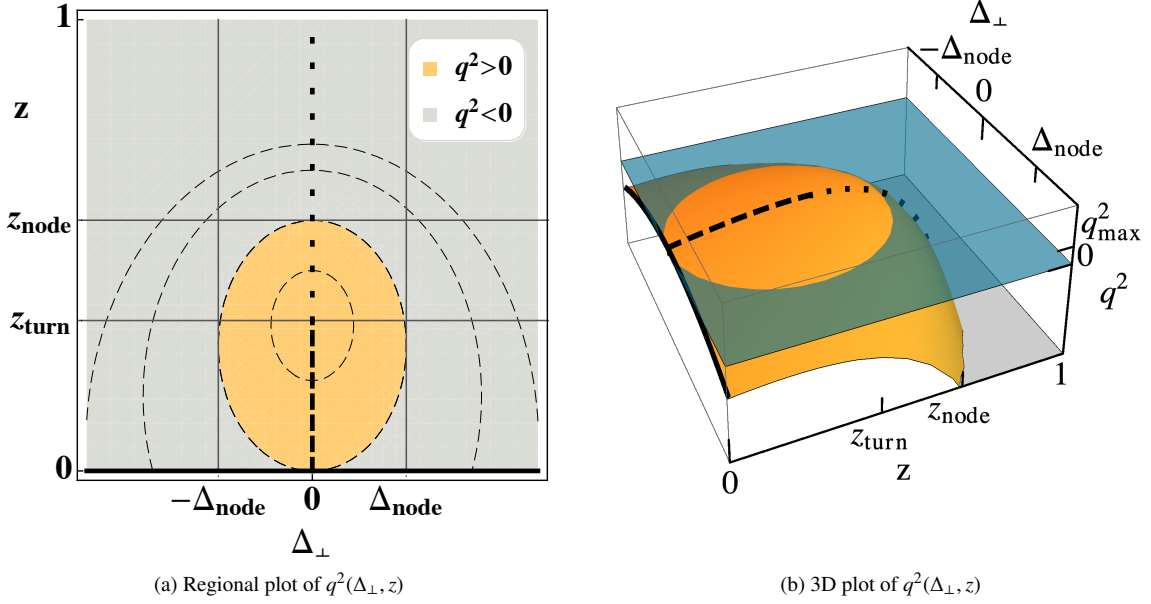


FIG. 2. Visualization of the Lorentz invariant momentum transfer squared q^2 as a function of z and $\vec{\Delta}_\perp$ at $\arg \vec{\Delta}_\perp = 0, \pi$. (a): regional plot of q^2 . The time-like region ($q^2 > 0$) is the orange oval shape, bounded by $\Delta_{\text{node}} = (m_A^2 - m_B^2)/2m_A$ and $z_{\text{node}} = 1 - m_B^2/m_A^2$. The space-like region ($q^2 < 0$) is in light gray. Contour lines of q^2 are indicated with thin dashed curves. The maximal value $q_{\text{max}}^2 = (m_A - m_B)^2$ occurs at ($z_{\text{turn}} = 1 - m_B/m_A, \Delta_\perp = 0$). (b): 3D plot of q^2 showing a convex shape in the (z, Δ_\perp) representation. The blue flat plane is the reference plane of $q^2 = 0$. In each figure, the Drell-Yan frame is shown as a thick solid line, and the longitudinal I and II frames are shown as thick dotted and thick dashed lines respectively.

$$\begin{aligned} \langle \psi_B(P, j, m_j) | J^\mu(0) | \psi_A(P', j', m'_j) \rangle_{n \rightarrow n} &= \sum_n f_n^2 \prod_{i=1}^n \sum_{s'_i, s_1, l'_i} \int_z \frac{dx'_1}{2x'_1} \int_0^1 \frac{dx'_{i(i \neq 1)}}{2x'_i} \int \frac{d^2 k'_{i\perp}}{(2\pi)^3} 2(2\pi)^3 \delta(\sum_{i=1}^n x'_i - 1) \delta^{(2)}(\sum_{i=1}^n \vec{k}'_{i\perp}) \\ &\times \psi_{n/B}^{(m_j)*}(\{x_i, \vec{k}_{i\perp}, s_i\}) f_{s_1, s'_1}^\mu \psi_{n/A}^{(m'_j)}(\{x'_i, \vec{k}'_{i\perp}, s'_i\}), \end{aligned} \quad (5)$$

where the EM current $f_{s_1, s'_1}^\mu = \bar{u}_{s'_1}(\kappa'_1) \gamma^\mu u_{s_1}(\kappa_1)$ if the struck parton is a quark, and $f_{s_1, s'_1}^\mu = \bar{v}_{s_1}(\kappa_1) \gamma^\mu v_{s'_1}(\kappa'_1)$ if the struck parton is an antiquark. l_i is the color index of the i -th parton and f_n is the color factor for the n -parton sector. The relative coordinates and constraint conditions of partons are

$$\begin{cases} x'_1 = x_1 + z(1 - x_1), \vec{k}'_{1\perp} = \vec{k}_{1\perp} + (1 - x_1)\vec{\Delta}_\perp, l_1 = l'_1, & \text{for the struck parton } (i = 1) \\ x'_i = x_i(1 - z), \vec{k}'_{i\perp} = \vec{k}_{i\perp} - x_i\vec{\Delta}_\perp, l_i = l'_i, s_i = s'_i, & \text{for the spectators } (i = 2, \dots, n). \end{cases} \quad (6)$$

In Sec. II B, we have shown that different choices of $(z, \vec{\Delta}_\perp)$ for the same q^2 could characterize different frames. Consider the z which is the lower bound of the range of x'_1 for the $n \rightarrow n$ matrix element in Eq. 5. As a consequence, increasing the value of z would reduce the overlap region of the two wavefunctions in the longitudinal direction. We illustrate this effect in Fig. 3 by visualizing the convoluted valence wavefunctions [28] at different $(z, \vec{\Delta}_\perp)$ with the same q^2 for the transition $J/\psi \rightarrow \eta_c + \gamma^{(*)}$. In the valence Fock sector, the light-front wavefunction can be written in the form of $\psi_{s\bar{s}/h}^{(m_j)}(\vec{k}_\perp, x)$

where (x, \vec{k}_\perp) is the relative coordinates of the quark. s represents the fermion spin projection in the x^- direction. Both the initial and final wavefunctions are plotted in the same (x, \vec{k}_\perp) space, where the initial state wavefunction would appear as being reshaped due to momentum transfer. We can see that the information from the wavefunction in the longitudinal direction is preserved most at minimal z .

For the $n + 2 \rightarrow n$ term, as in Fig. 1(b), a quark and an antiquark from the initial state annihilate into a photon, thus the electromagnetic current matrix element takes the form

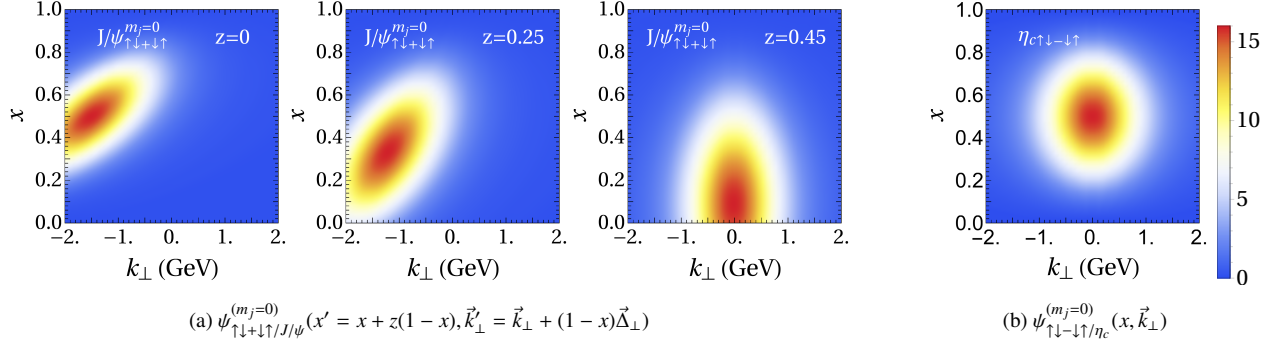


FIG. 3. The valence light-front wavefunctions of mesons as they contribute (see Eq. (5)) to the convolution in the transition $J/\psi \rightarrow \eta_c + \gamma^{(*)}$ at $q^2 = -3\text{GeV}^2$ in different frames. According to Eq. (5), in this $2 \rightarrow 2$ parton-number-conserving term, the initial state wavefunction of J/ψ would appear shifted and stretched to overlap with the final state wavefunction of η_c , when plotted on the (x, \vec{k}_{\perp}) space. Shown in (a), the wavefunction of J/ψ is shaped differently at different $(z, \vec{\Delta}_{\perp})$, i.e. in different frames. The longitudinal dimension is preserved most in the Drell-Yan frame where $z = 0$. At larger z , the information in the longitudinal region is reduced, and the transverse shift becomes smaller. The largest z is achieved when $\Delta_{\perp} = 0$ in the longitudinal frame, in this case, $z = 0.45$. Plotted in (b) is the wavefunction of η_c . All light-front wavefunctions what we employ are calculated by Ref. [28] and here we only plot the dominant spin components for the purpose of illustration.

$$\begin{aligned} \langle \psi_B(P, j, m_j) | J^{\mu} | \psi_A(P', j', m'_j) \rangle_{n+2 \rightarrow n} &= \sum_n f_n f_{n+2} \prod_{i=1}^{n+2} \sum_{s'_i, l'_i} \int_0^z \frac{dx'_1}{2x'_1} \int_0^1 \frac{dx'_{i(i \neq 1,2)}}{2x'_i} \int \frac{d^2 k'_{i\perp}}{(2\pi)^3} 2(2\pi)^3 \delta(\sum_{i=1}^{n+2} x'_i - 1) \delta^{(2)}(\sum_{i=1}^{n+2} \vec{k}'_{i\perp}) \\ &\times \psi_{n/B}^{(m_j)*}(\{x_i, \vec{k}_{i\perp}, s_i\}) f_{s'_1, s'_2}^{\mu} \psi_{n+2/A}^{(m'_j)}(\{x'_i, \vec{k}'_{i\perp}, s'_i\}), \end{aligned} \quad (7)$$

where the EM current is $f_{s'_1, s'_2}^{\mu} = \bar{v}_{s'_1}(\kappa'_2) \gamma^{\mu} u_{s'_2}(\kappa'_1)$ and the parton coordinates/constraints are

$$\begin{cases} x'_1, \vec{k}'_1, & \text{for the struck quark} \\ x'_2 = z - x'_1, \vec{k}'_2 = -\vec{k}'_1 + \vec{\Delta}_{\perp}, l'_2 = l'_1, & \text{for the struck anti-quark} \\ x'_{i+2} = x_i(1-z), \vec{k}'_{i+2\perp} = \vec{k}_{i\perp} - x_i \vec{\Delta}_{\perp}, l_i = l'_{i+2}, s_i = s'_{i+2}, & \text{for the spectators } (i = 1, \dots, n). \end{cases} \quad (8)$$

The frame parameter z is now the upper bound of the range of x'_1 , suggesting that decreasing the value of z might reduce the contribution of the $n+2 \rightarrow n$ transition to the full transition form factor. However, even at $z = 0$, this parton-number-non-conserving term may yield a non-zero value, by generating zero-mode $\delta(x)$ terms [16, 17, 35, 36]. In the space-like region, the Drell-Yan frame always has the minimal $z = 0$. In the time-like region, it is the longitudinal-II frame that takes the smallest z . When the $n+2 \rightarrow n$ contribution is not accessible, which happens when the light-front wavefunctions are solved in a truncated Fock space, using those minimal- z frames seems advantageous in suppressing the parton-number-non-conserving contribution. This observation suggests optimal frames for our meson systems solved from light-front Hamiltonian in the valence Fock sector.

In the valence Fock sector, the transition amplitude of $\psi_A \rightarrow \psi_B$ with the current operator $J^{\mu}(x) = \bar{\psi}(x) \gamma^{\mu} \psi(x)$ now contains only two contributions, one from the photon coupling to the quark and the other from the photon coupling to the antiquark. For quarkonia, the two terms are equal by charge conjugation. For convenience, in calculating the transition form factor, we

only consider the photon coupling to the quark and the charge is not included. That is, we compute $\hat{V}(q^2)$ which is related to $V(q^2)$ by $\hat{V}(q^2) = V(q^2)/(2eQ_f)$ where Q_f is the dimensionless fractional charge of the quark.

In our previous work [22], we have shown that for calculations with light-front wavefunctions in the valence Fock sector, using the transverse current $J^R (\equiv J^x + iJ^y)$ with the $m_j = 0$ state of the vector meson is preferred for the transition form factor $V(q^2)$, as in Eq. (9). We will adopt this choice for the purpose of studying the frame dependence in this work. Therefore, we employ

$$\langle \mathcal{P}(P) | J^R(0) | \mathcal{V}(P', m_j) \rangle = \frac{2V(q^2)}{m_{\mathcal{P}} + m_{\mathcal{V}}} im_{\mathcal{V}} P^+ \left[\frac{P^R}{P^+} - \frac{P'^R}{P'^+} \right]. \quad (9)$$

The light-front wavefunction representation of the transition form factor $\hat{V}(q^2)$, extracted according to the expression

in Eq. (9), follows as

$$\hat{V}(q^2) = -i \frac{m_V + m_P}{2m_V \Delta^R} \sum_{\bar{s}} \int_0^1 \frac{dx}{2x(1-x)} \int \frac{d^2 \vec{k}_{\perp}}{(2\pi)^3} \frac{2}{\sqrt{x(1-z)[x+z(1-x)]^3}} \left[\psi_{\uparrow \bar{s}/P}^*(\vec{k}_{\perp}, x) \psi_{\uparrow \bar{s}/V}^{(m_j=0)}(\vec{k}'_{\perp}, x') \right. \\ \left. \times (zk^R - x\Delta^R) + \psi_{\downarrow \bar{s}/P}^*(\vec{k}_{\perp}, x) \psi_{\uparrow \bar{s}/V}^{(m_j=0)}(\vec{k}'_{\perp}, x') m_{qz} \right]. \quad (10)$$

We will numerically probe the frame dependence of the transition form factor through a dense sampling of kinematically available frames within $(z, \vec{\Delta}_{\perp})$ for any given q^2 . We will also try to see if our suggested frames, those with minimal- z , provide a better results than other frames, when compared with available experimental data.

III. RESULTS: THE M1 TRANSITIONS IN HEAVY QUARKONIA

We adopt light-front wavefunctions of heavy quarkonia from recent works [27, 28] in the BLFQ approach [26]. The effective Hamiltonian extends the holographic QCD [37] by introducing the one-gluon exchange interaction with a running coupling, the constituent masses for the quarks and a longitudinal confining interaction [38]. The obtained light-front wavefunctions have been used to produce several observables and are in reasonable agreement with experiments and with other theoretical approaches [25, 39–42]. We have also used these light-front wavefunctions to address radiative transitions in a previous work [22]. The previous work studied the transition form factor in the space-like region in the Drell-Yan frame, and suggested a preferred current component for practical calculations. The present work extends the calculation to the full kinematic region and all possible frame choices.

In this model, the light-front wavefunctions are solved in the valence Fock sector using a basis function representation, where the truncations in the Fock space and the basis space could introduce a violation of Lorentz symmetry. However, such a violation turned out to be very small in terms of the meson mass spread at different magnetic projections, as well as in the elastic form factors for mesons at different frames [25]. It is therefore worthwhile to examine how the transition form factors exhibit Lorentz symmetry violation as measured by their frame-dependence.

The light-front wavefunction in a basis function representation reads:

$$\psi_{\bar{s}s/h}^{(m_j)}(\vec{k}_{\perp}, x) = \sum_{n,m,l} \psi_h(n, m, l, s, \bar{s}) \phi_{nm}\left(\frac{\vec{k}_{\perp}}{\sqrt{x(1-x)}}\right) \chi_l(x). \quad (11)$$

In the transverse direction, the 2D harmonic oscillator (HO) function ϕ_{nm} is adopted as the basis. In the longitudinal direction, we use the modified Jacobi polynomial χ_l as the basis. m is the orbital angular momentum projection, related to

the total angular momentum projection as $m_j = m + s + \bar{s}$, which is conserved by the Hamiltonian. The basis space is truncated by their reference energies in dimensionless units: $2n + |m| + 1 \leq N_{\max}$ and $0 \leq l \leq L_{\max}$. As such, the N_{\max} -truncation provides a natural pair of UV and IR cutoffs: $\Lambda_{\perp,UV} \simeq \kappa \sqrt{N_{\max}}$, $\lambda_{\perp,IR} \simeq \kappa / \sqrt{N_{\max}}$, where κ is the oscillator basis energy scale parameter as well as the confining strength parameter. L_{\max} represents the resolution of the basis in the longitudinal direction $\Delta x \approx L_{\max}^{-1}$. It also provides a pair of UV and IR cutoffs according to Eq. (4): $\Lambda_{z,UV} \simeq m_h \sqrt{L_{\max}}$, $\lambda_{z,IR} \simeq m_h / \sqrt{L_{\max}}$ ($m_h \approx m_A, m_B$). See Ref. [28] for details on basis functions and parameter values. The light-front wavefunctions are calculated at $N_{\max} = L_{\max} = 8, 16, 24$ and 32 . For our purposes, we mainly concentrate on results obtained at $N_{\max} = L_{\max} = 32$. In this basis, the largest supported $|q^2|$ is $31 \text{ GeV}^2 (44 \text{ GeV}^2)$ for charmonia (bottomonia), and beyond these cutoffs, the LFWFs are dominated by the asymptotics of the basis.

A. The transition form factors in different frames

Figures 4 and 5 show numerical results for selected pseudoscalar-vector transition form factors for charmonia and bottomonia below their respective open-flavor thresholds. Those lowest states are the primary focii of several investigations [3, 43–47]. They have been measured in experiments [1], and their transitions are more readily detected with good statistics than higher excited states. Moreover, with their experimental masses, we have an entire landscape of frames in the $(z, \vec{\Delta}_{\perp})$ parameter space according to Eq. (4). The solid curve represents the Drell-Yan frame, the dotted and the dashed curves represent the two branches of the longitudinal frame, longitudinal I and longitudinal II respectively. The shaded areas represent all other frames with different z and Δ_{\perp} . We also compare $\hat{V}(0)$ obtained in different frames with available experimental data from the Particle Data Group (PDG) [1] in Table. I.

TABLE I. Comparison of $\hat{V}(0)$ from available experimental data and the BLFQ calculations in the limiting frames. Values from PDG [1] are converted from their decay widths according to Eq. (2). The BLFQ results are calculated using meson wavefunctions obtained at $N_{\max} = L_{\max} = 32$. The Drell-Yan/longitudinal II is the preferred result, and the difference between it and the longitudinal I quantifies the uncertainty resulting from frame dependence.

$\hat{V}(0)$	PDG [1]	BLFQ	
		Drell-Yan/long-II	long-I
$J/\psi(1S) \rightarrow \eta_c(1S)\gamma$	1.56(19)	2.02	2.12
$\eta_c(2S) \rightarrow J/\psi(1S)\gamma$...	-0.019	0.29
$\psi(2S) \rightarrow \eta_c(1S)\gamma$	0.100(8)	0.29	0.46
$\psi(2S) \rightarrow \eta_c(2S)\gamma$	2.52(91)	2.09	2.14
$\Upsilon(1S) \rightarrow \eta_b(1S)\gamma$...	2.01	2.03
$\eta_b(2S) \rightarrow \Upsilon(1S)\gamma$...	-0.052	0.20
$\Upsilon(2S) \rightarrow \eta_b(1S)\gamma$	0.070(14)	0.13	0.35
$\Upsilon(2S) \rightarrow \eta_b(2S)\gamma$...	2.02	2.03

For the transition form factor of the *allowed* transition, i.e. $\psi_A(nS) \rightarrow \psi_B(nS)\gamma$, ($\psi_A, \psi_B = \mathcal{V}, \mathcal{P}$ or \mathcal{P}, \mathcal{V}), as in Fig. 4, there are no crossings between the curves of the longitudinal frame and the Drell-Yan frame. In these cases, the results from all other frames are represented by the enclosed shaded area. The frame dependence is relatively small, no more than a 5% spread at $q^2 = 0$, as in Table. I. For the transition form factor of the *hindered* transitions, i.e. $\psi_A(nS) \rightarrow \psi_B(n'S)\gamma$ ($n' \neq n$), ($\psi_A, \psi_B = \mathcal{V}, \mathcal{P}$ or \mathcal{P}, \mathcal{V}), as in Fig. 5, the curves of the longitudinal frame and the Drell-Yan frame cross each other, and their joined lower bound forms the lower bound for the results from all other frames. The upper bound, however, envelops the Drell-Yan and the longitudinal results. The frame dependence of these hindered transitions is very strong, indicating major sensitivity to the Lorentz symmetry breaking. This sensitivity seems understandable since these weaker transitions result from cancellations coming from different regions of integration.

We also compare charmonia and bottomonia at corresponding transition modes in Figs. 4 and 5. Such comparisons suggest that the frame dependence tends to be reduced for heavier systems, presumably due to the overall reduction in relativistic effects.

It is natural to ask how frame dependence may be sensitive to the BLFQ basis truncation applied to these valence Fock space calculations. For this purpose, we present transition form factors from different basis truncations in Fig. 6. A trend towards convergence with increasing basis cutoff is observed in both the Drell-Yan and the longitudinal frames. The frame dependence indicated by the shaded regions is shrinking slightly with increasing basis cutoff but Lorentz symmetry breaking effects remain visible even at the highest basis cutoffs.

From those results, we observe that the frame dependence of the transition form factor can be characterized by the two limits, the Drell-Yan and the longitudinal frames. Transitions with excitations in the lighter system (e.g. $\eta_c(2S) \rightarrow J/\psi(1S)\gamma$) admit the largest frame dependence, implying a stronger sensitivity to the Fock sector truncation. Our suggested frames for the calculation in the valence Fock sector, the Drell-Yan and the longitudinal-II frames, provide values of $\hat{V}(0)$ that are closer to the experimental data, as seen in Table. I.

B. The electromagnetic Dalitz decay

The effective mass spectrum of the lepton pair in the Dalitz decay can be obtained from the corresponding transition form factor according to Eqs. (2) and (3). The results of $d\Gamma(\psi_A \rightarrow \psi_B l^+ l^-) / dq^2$ for eight selected decays are shown in Fig. 7. The frame dependence is barely visible in the allowed transitions as in the top four panels, but very substantial in the hindered transitions as in the bottom four panels. Such different sensitivities to frames can be expected in light of the sensitivities observed for the transition form factors in the time-like region. The allowed transitions are between states with similar spatial wavefunctions (e.g. $J/\psi(1S) \rightarrow \eta_c(1S)e^+e^-$), whereas the

hindered transitions are between states with nearly orthogonal spatial parts (e.g. $\psi(2S) \rightarrow \eta_c(1S)e^+e^-$). Therefore in the latter cases, the transition form factors and thus the leptonic widths would admit strong cancellations between positive and negative contributions, and thus become more sensitive to the finer details of light-front wavefunctions.

IV. SUMMARY AND OUTLOOK

We have introduced the M1 transition form factor on the light front in a general frame. We analyzed the contributions from the parton-number-conserving term ($n \rightarrow n$) and the non-conserving term ($n+2 \rightarrow n$) in different frames, and suggested that frames with minimal z values could suppress the latter. Therefore, the minimal- z frames, i.e. the Drell-Yan and the longitudinal-II frames, are preferred for calculating transition form factors in the valence Fock sector.

We then looked into the heavy quarkonia system and showed that, using light-front wavefunctions from the valence Fock sector, the transition form factor admits moderate frame dependence in the case of allowed transitions. For the case of hindered transitions, we find that the frame dependence is more severe. Our results from different frames fall between the two special frames, the Drell-Yan and the longitudinal frames, a pattern also observed in the study of elastic form factors [25]. In the space-like region, the Drell-Yan and the longitudinal-I frames form two limits, while in the time-like region, the limits become the two branches of the longitudinal frame (referred as longitudinal I and II). We employed the difference of results in the Drell-Yan and the longitudinal frames as a metric for the violation of the Lorentz symmetry due to Fock space truncation.

With the transition form factor in the time-like region, we obtained the decay widths of the associated Dalitz decay and use the frame difference as an uncertainty for the result. We hope that the comparison of our predictions with future experiments could help justify our choice of the preferred frames for valence Fock sector calculations. By exhibiting frame dependence in these form factors and decay widths, we motivate solving quarkonia systems in higher Fock sectors [48, 49] and providing a more complete description with increasingly precise treatments of the Lorentz symmetry.

We expect that by considering contributions from higher Fock sectors, this frame dependence would eventually vanish. As we have discussed in Sec. II, in terms of the transition form factor, the contribution from the valence sector and that from the higher sectors are different in different frames, but the full result (the summation of the two) should be invariant. The comparison of the future full transition form factor to the valence result in different frames, as presented here, could verify our deduction on the suggested frames. In practical calculations, if taking into account the higher Fock sector contribution does not resolve all the frame dependence, the residue is likely caused by approximations in modeling the Hamiltonian and numerical uncertainties. Checking the frame dependence could still provide a measurement on the violation of the Lorentz symmetry for the phenomenological model of

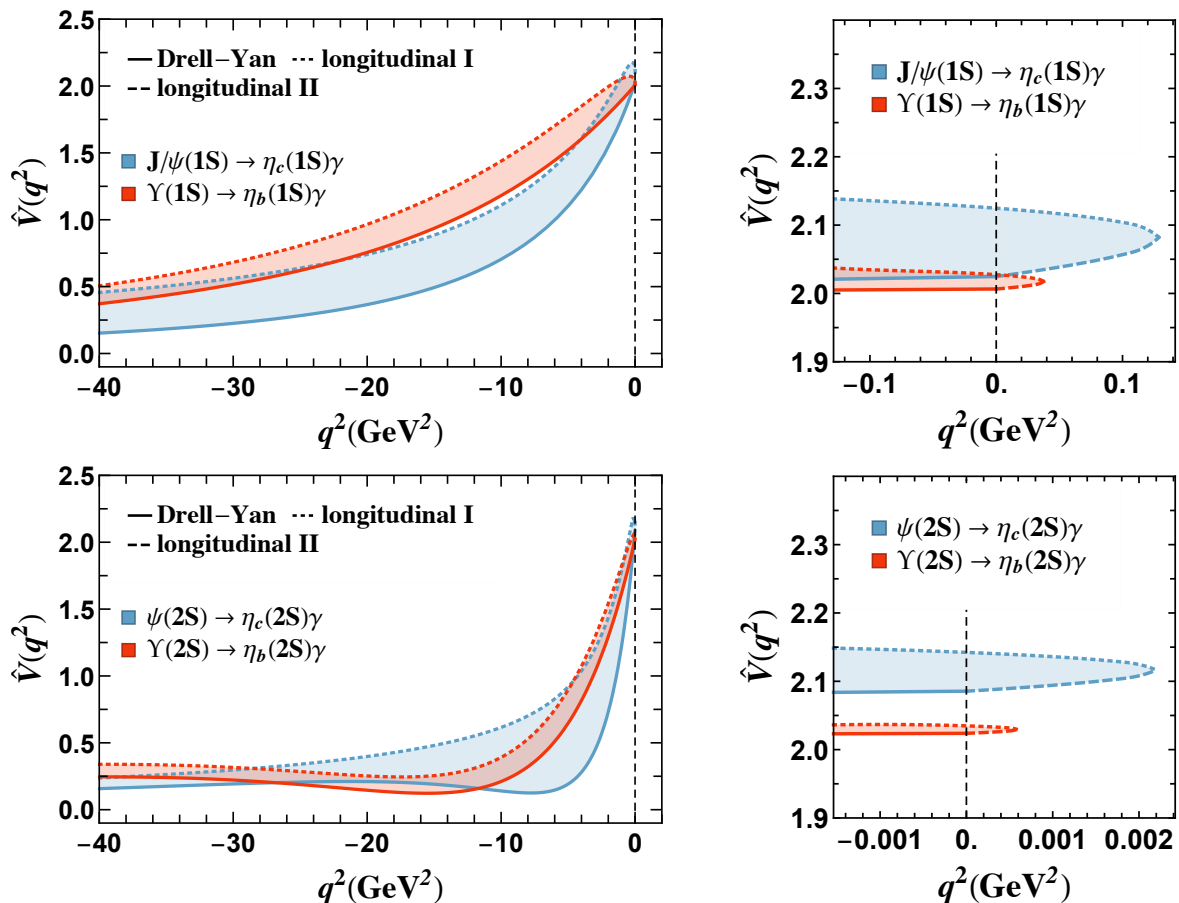


FIG. 4. The transition form factor of the transition $\mathcal{V}(nS) \rightarrow \mathcal{P}(nS)\gamma$ of charmonia (blue curves/shades) and bottomonia (red curves/shades), calculated with light-front wavefunctions at $N_{\max} = L_{\max} = 32$ basis truncation. Meson masses are taken from experimental data [1] in defining the frames according to Eq. (4). The solid curves represent the Drell-Yan frame while the other curves represent the longitudinal I (dotted lines) and II (dashed lines) frames. The shaded areas represent the results from all other frames. The left panel shows the transition form factor at a larger scale of q^2 , and the right panel focuses on the small q^2 region.

the system.

It should be noted that though we take heavy quarkonia as a concrete study object in this paper, the formalism of the transition form factors in different frames also applies to light mesons and could be extended to other systems such as baryons.

ACKNOWLEDGMENTS

We wish to thank Shaoyang Jia, Tobias Frederico, Shuo Tang, Wenyang Qian, Anji Yu, Xingbo Zhao, Ho-Meoyng

Choi and Chueng-Ryong Ji for valuable discussions. This work was supported in part by the US Department of Energy (DOE) under Grant Nos. DE-FG02-87ER40371, DE-SC0018223 (SciDAC-4/NUCLEI), DE-SC0015376 (DOE Topical Collaboration in Nuclear Theory for Double-Beta Decay and Fundamental Symmetries). This research used resources of the National Energy Research Scientific Computing Center (NERSC), a U.S. Department of Energy Office of Science User Facility operated under Contract No. DE-AC02-05CH11231.

[1] M. Tanabashi *et al.* (Particle Data Group), Phys. Rev. **D98**, 030001 (2018).

[2] N. Brambilla, Y. Jia, and A. Vairo, Phys. Rev. **D73**, 054005 (2006), arXiv:hep-ph/0512369 [hep-ph].

[3] G. C. Donald, C. T. H. Davies, R. J. Dowdall, E. Follana, K. Hornbostel, J. Koponen, G. P. Lepage, and C. McNeile, Phys. Rev. **D86**, 094501 (2012), arXiv:1208.2855 [hep-lat].

[4] D. Ebert, R. N. Faustov, and V. O. Galkin, Phys. Rev. **D67**, 014027 (2003), arXiv:hep-ph/0210381 [hep-ph].

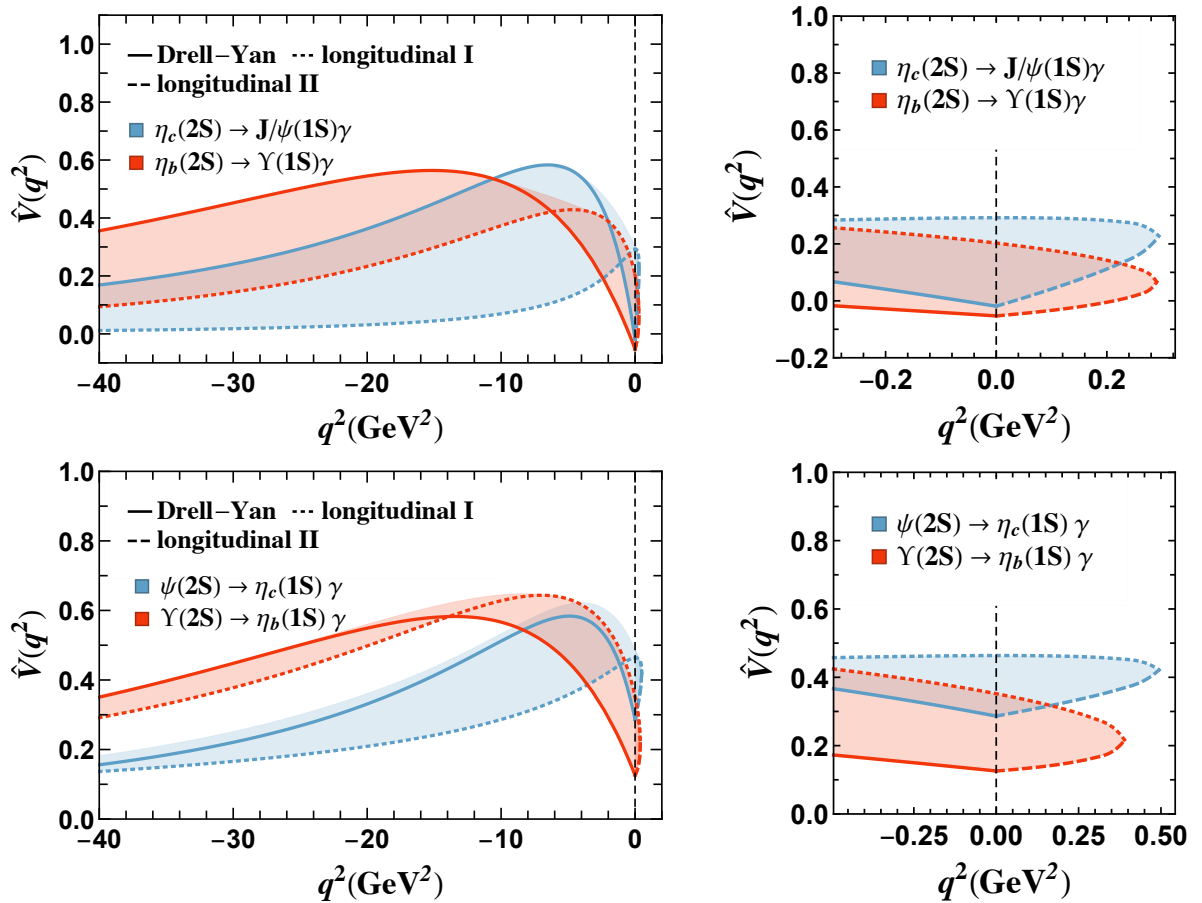


FIG. 5. The transition form factor of the transition $\psi_A(2S) \rightarrow \psi_B(1S)\gamma$ ($\psi_A, \psi_B = \mathcal{V}, \mathcal{P}$ or \mathcal{P}, \mathcal{V}) of charmonia (blue curves/shades) and bottomonia (red curves/shades), calculated with light-front wavefunctions at $N_{\max} = L_{\max} = 32$ basis truncation. Meson masses are taken from experimental data [1] for defining the frames according to Eq. (4). The solid curves represent the Drell-Yan frame while the other curves represent the longitudinal I (dotted lines) and II (dashed lines) frames. The shaded areas represent the results from all other frames. The left panel shows the transition form factor at a larger scale of q^2 , and the right panel focuses on the small q^2 region.

- [5] T. Barnes, S. Godfrey, and E. S. Swanson, *Phys. Rev.* **D72**, 054026 (2005), arXiv:hep-ph/0505002 [hep-ph].
- [6] A. Pineda and J. Segovia, *Phys. Rev.* **D87**, 074024 (2013), arXiv:1302.3528 [hep-ph].
- [7] R. H. Dalitz, *Proc. Phys. Soc.* **A64**, 667 (1951).
- [8] A. Anastasi *et al.* (KLOE-2), *Phys. Lett.* **B757**, 362 (2016), arXiv:1601.06565 [hep-ex].
- [9] M. N. Achasov *et al.*, *Phys. Lett.* **B504**, 275 (2001).
- [10] D. Babusci *et al.* (KLOE-2), *Phys. Lett.* **B742**, 1 (2015), arXiv:1409.4582 [hep-ex].
- [11] R. R. Akhmetshin *et al.* (CMD-2), *Phys. Lett.* **B613**, 29 (2005), arXiv:hep-ex/0502024 [hep-ex].
- [12] P. Adlarson *et al.*, *Phys. Rev.* **C95**, 035208 (2017), arXiv:1609.04503 [hep-ex].
- [13] M. Ablikim *et al.* (BESIII), *Phys. Rev.* **D89**, 092008 (2014), arXiv:1403.7042 [hep-ex].
- [14] M. Ablikim *et al.* (BESIII), *Phys. Lett.* **B783**, 452 (2018), arXiv:1803.09714 [hep-ex].
- [15] M. Sawicki, *Phys. Rev.* **D46**, 474 (1992).
- [16] J. P. B. C. de Melo, J. H. O. Sales, T. Frederico, and P. U. Sauer, *Proceedings, 15th International IUPAP Conference on Few body problems in physics (FB15): Groningen, Netherlands, July 22-26, 1997*, *Nucl. Phys.* **A631**, 574C (1998), arXiv:hep-ph/9802325 [hep-ph].
- [17] S. J. Brodsky and D. S. Hwang, *Nucl. Phys.* **B543**, 239 (1999), arXiv:hep-ph/9806358 [hep-ph].
- [18] B. L. G. Bakker, H.-M. Choi, and C.-R. Ji, *Phys. Rev.* **D67**, 113007 (2003), arXiv:hep-ph/0303002 [hep-ph].
- [19] J. Carbonell, B. Desplanques, V. A. Karmanov, and J. F. Mathiot, *Phys. Rept.* **300**, 215 (1998), arXiv:nucl-th/9804029 [nucl-th].
- [20] A. T. Suzuki, J. H. Sales, and L. A. Soriano, *Phys. Rev.* **D88**, 025036 (2013), arXiv:1209.4681 [hep-th].
- [21] D. Melikhov and S. Simula, *Phys. Rev.* **D65**, 094043 (2002), arXiv:hep-ph/0112044 [hep-ph].
- [22] M. Li, Y. Li, P. Maris, and J. P. Vary, *Phys. Rev.* **D98**, 034024 (2018), arXiv:1803.11519 [hep-ph].
- [23] H.-Y. Cheng, C.-Y. Cheung, and C.-W. Hwang, *Phys. Rev.* **D55**, 1559 (1997), arXiv:hep-ph/9607332 [hep-ph].
- [24] C.-R. Ji and C. Mitchell, *Phys. Rev.* **D62**, 085020 (2000).
- [25] Y. Li, P. Maris, and J. P. Vary, *Phys. Rev.* **D97**, 054034 (2018), arXiv:1712.03467 [hep-ph].
- [26] J. P. Vary, H. Honkanen, J. Li, P. Maris, S. J. Brodsky, A. Harindranath, G. F. de Teramond, P. Sternberg, E. G. Ng, and C. Yang, *Phys. Rev.* **C81**, 035205 (2010), arXiv:0905.1411 [nucl-th].

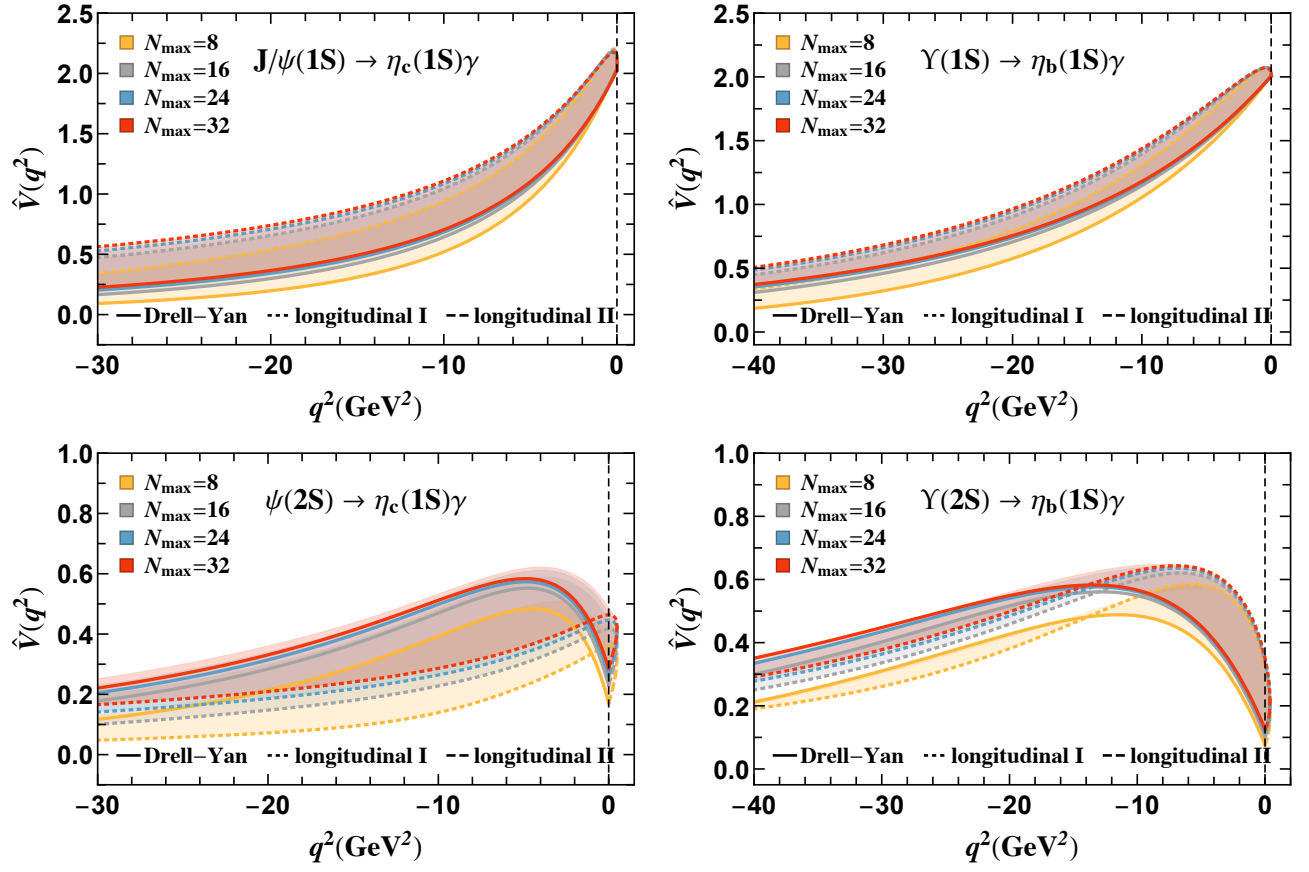


FIG. 6. The transition form factors for charmonia (left panels) and bottomonia (right panels) with different basis truncations. Meson masses are taken from experimental data [1] in defining the frames according to Eq. (4). The solid curves represent the Drell-Yan frame while the other curves represent the longitudinal I (dotted lines) and II (dashed lines) frames. The shaded areas represent the results from all other frames.

- [27] Y. Li, P. Maris, X. Zhao, and J. P. Vary, Phys. Lett. **B758**, 118 (2016), arXiv:1509.07212 [hep-ph].
- [28] Y. Li, P. Maris, and J. P. Vary, Phys. Rev. **D96**, 016022 (2017), arXiv:1704.06968 [hep-ph].
- [29] J. J. Dudek, R. G. Edwards, and D. G. Richards, Phys. Rev. **D73**, 074507 (2006), arXiv:hep-ph/0601137 [hep-ph].
- [30] L. G. Landsberg, Phys. Rept. **128**, 301 (1985).
- [31] S. Simula, Phys. Rev. **C66**, 035201 (2002), arXiv:nucl-th/0204015 [nucl-th].
- [32] D. Melikhov, Phys. Rev. **D53**, 2460 (1996), arXiv:hep-ph/9509268 [hep-ph].
- [33] W. Jaus, Phys. Rev. **D53**, 1349 (1996), [Erratum: Phys. Rev.D54,5904(1996)].
- [34] N. Isgur and C. H. Llewellyn Smith, Nucl. Phys. **B317**, 526 (1989).
- [35] S.-J. Chang, R. G. Root, and T.-M. Yan, Phys. Rev. **D7**, 1133 (1973).
- [36] M. Burkardt, Nucl. Phys. **A504**, 762 (1989).
- [37] S. J. Brodsky, G. F. de Teramond, H. G. Dosch, and J. Erlich, Phys. Rept. **584**, 1 (2015), arXiv:1407.8131 [hep-ph].
- [38] P. Wiecki, Y. Li, X. Zhao, P. Maris, and J. P. Vary, Phys. Rev. **D91**, 105009 (2015), arXiv:1404.6234 [nucl-th].
- [39] G. Chen, Y. Li, P. Maris, K. Tuchin, and J. P. Vary, Phys. Lett. **B769**, 477 (2017), arXiv:1610.04945 [nucl-th].
- [40] S. Leitão, Y. Li, P. Maris, M. T. Peña, A. Stadler, J. P. Vary, and E. P. Biernat, Eur. Phys. J. **C77**, 696 (2017), arXiv:1705.06178 [hep-ph].
- [41] L. Adhikari, Y. Li, M. Li, and J. P. Vary, Phys. Rev. **C99**, 035208 (2019), arXiv:1809.06475 [hep-ph].
- [42] G. Chen, Y. Li, K. Tuchin, and J. Vary, to be published (2018), arXiv:1811.01782 [nucl-th].
- [43] W.-J. Deng, H. Liu, L.-C. Gui, and X.-H. Zhong, Phys. Rev. **D95**, 074002 (2017), arXiv:1607.04696 [hep-ph].
- [44] C. Hughes, R. J. Dowdall, C. T. H. Davies, R. R. Horgan, G. von Hippel, and M. Wingate, Phys. Rev. **D92**, 094501 (2015), arXiv:1508.01694 [hep-lat].
- [45] D. Bečirević and F. Sanfilippo, JHEP **01**, 028 (2013), arXiv:1206.1445 [hep-lat].
- [46] S. Godfrey and J. L. Rosner, Phys. Rev. **D64**, 074011 (2001), [Erratum: Phys. Rev.D65,039901(2002)], arXiv:hep-ph/0104253 [hep-ph].
- [47] S. Godfrey and K. Moats, Phys. Rev. **D92**, 054034 (2015), arXiv:1507.00024 [hep-ph].
- [48] Y. Li, V. A. Karmanov, P. Maris, and J. P. Vary, Phys. Lett. **B748**, 278 (2015), arXiv:1504.05233 [nucl-th].
- [49] V. A. Karmanov, Y. Li, A. V. Smirnov, and J. P. Vary, Phys. Rev. **D94**, 096008 (2016), arXiv:1610.03559 [hep-th].

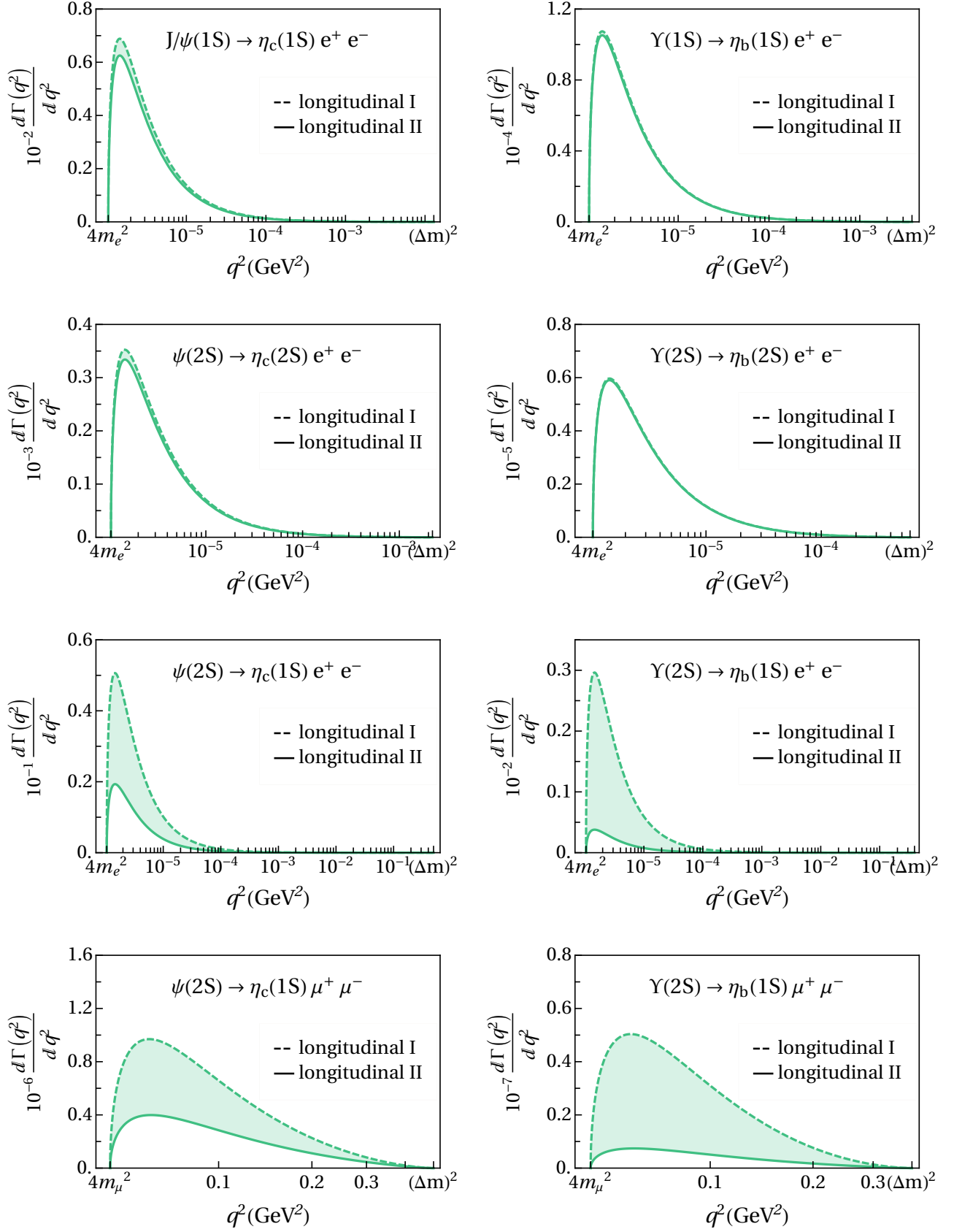


FIG. 7. The effective mass spectrum of the lepton pairs in the Dalitz decays for charmonia (left panels) and bottomonia (right panels). The dashed and solid curves represent the longitudinal I and II frames respectively. The shaded areas represent the results from all other frames. $\Delta m^2 = (m_A - m_B)^2$ is the square of the mass difference between the initial and the final mesons. Meson masses are taken from experimental data [1].